Role of Glutamine-61 in the Hydrolysis of GTP by p21$^{H\text{-}ras}$: An Experimental and Theoretical Study†

M. Frech,‡,§ T. A. Darden,*,‖ L. G. Pedersen,‖,⊥ C. K. Foley,▽ P. S. Charifson,+ M. W. Anderson,‖ and A. Wittinghofer§

Institute de Pharmacologie Moleculaire et Cellulaire, Centre National de la Recherche Scientifique, Valbonne, France, Abteilung für Strukturelle Biologie, Max-Planck-Institut für Molekulare Physiologie, Rheinlanddamn 201, 44139 Dortmund, FRG, National Institute of Environmental Health Sciences, Research Triangle Park, North Carolina 27709, Department of Chemistry, University of North Carolina at Chapel Hill, Chapel Hill, North Carolina 27514, Cray Research, Inc., P.O. Box 12746, Research Triangle Park, North Carolina 27709, and Glaxo Inc., 5 Moore Drive, Research Triangle Park, North Carolina 27709

Received August 16, 1993; Revised Manuscript Received November 29, 1993®

ABSTRACT: The active GTP-bound form of p21^{ras} is converted to the biologically inactive GDP-bound form by enzymatic hydrolysis and this function serves to regulate the wild-type *ras* protein. The side chain of the amino acid at position 61 may play a key role in this hydrolysis of GTP by p21. Experimental studies that define properties of the Q61E mutant of p21$^{H\text{-}ras}$ are presented along with supporting molecular dynamics simulations. We find that under saturating concentrations of GTP the Q61E mutant of p21$^{H\text{-}ras}$ has a 20-fold greater rate of intrinsic hydrolysis (k_{cat} = 0.57 min^{-1}) than the wild type. The affinity of the Q61E variant for GTP (K_d = 115 μM) is much lower than that of the wild type. GTPase activating protein does not activate the variant. From molecular dynamics simulations, we find that both the wild type and Q61E mutant have the residue 61 side chain in transient contact with a water molecule that is well-positioned for hydrolytic attack on the γ phosphate. Thr-35 also is found to form a transient hydrogen bond with this critical water. These elements may define the catalytic complex for hydrolysis of the GTP [Pai et al. (1990) *EMBO J. 9,* 2351]. Similarly, the G12P mutant, which also has an intrinsic hydrolysis rate similar to the wild type, is found to form the same complex in simulation. In contrast, molecular dynamics analysis of the mutants G12R, G12V, and Q61L, which have much lower intrinsic rates than the wild-type p21, do not show this complex. Thus, the experimental data for intrinsic hydrolysis rates and the molecular dynamics simulations support the view that the residue 61 side chain is involved in activating a water molecule in the GTP hydrolysis mechanism.

The *ras* genes (N-, K- and H-*ras*) encode the p21 *ras* family of proteins which have been implicated in cellular growth control (Bourne et al., 1990, 1991). Mutations in these membrane-bound cytoplasmic proteins, particularly at positions 12 and 61, have been found in many mammalian tumors (Barbacid, 1987; Spandidos, 1989; Bos, 1989). It has become clear that the GTP-bound[1] state of the oncogenic proteins has a much longer half-life than that of the analogous wild type proteins and that this state is then relatively impervious to GTP hydrolysis activation by GAP (GTPase activating protein) (Krengel et al., 1990). A growth signal is apparently turned on while the protein (wild type or mutant) is in the GTP-bound state. The oncogenic mutant forms remain in the active GTP-bound state much longer than the wild type and thus the continual transmission of the signal is responsible, at least in part, for the oncogenic properties. Other factors such as proteins which modulate the rate of exchange of GDP/GTP (Downward et al., 1990; West et al., 1990; Wolfman & Macara, 1990) may also affect observations of transformation efficiency.

Previous structural studies (Pai et al., 1990; Prive et al., 1992) have focused on p21 in its GDP- and GTP-bound state. Fortunately, the wild-type p21$^{H\text{-}ras}$ protein has an intrinsic hydrolysis rate which, although much slower than the GAP-induced rate, has provided a reasonable starting point for combined kinetic and structural studies. Because the intrinsic hydrolysis also takes place in the crystalline complex (Schlichting et al., 1989), it is necessary to study the p21–GTP complex using analogs of GTP which presumably maintain the structural integrity of the complex but are nonhydrolyzable. For instance, Pai et al. (1990) presented a 1.35-Å resolution crystal structure of the complex in which the bridging oxygen between the β and γ phosphates of GTP was replaced by an -NH- group. Likewise, Prive et al. (1992), recently reported a 1.95-Å resolution structure of a p21–GTP complex in which the ethereal oxygen was replaced by a -CH_2- group. The Pai et al. (1990) structure has also been used as the starting point for a molecular dynamics study of the solvated complex (Foley et al., 1992), whereas the Prive et al. (1992) structure has served as the model for an empirical valence bond study by Langen et al. (1992).

Whereas these crystallographic studies find areas of agreement, they differ in the subsequent mechanisms for how the hydrolysis takes place. Pai et al. (1990) propose, on the

† This work was supported in part by Grant HL27995 from the National Heart, Blood and Lung Institute.

* Author to whom correspondence should be addressed.
‡ CNRS.
§ Max-Planck-Institut für Molekulare Physiologie.
‖ NIEHS.
⊥ UNC—Chapel Hill.
▽ Cray Research.
+ Glaxo.

® Abstract published in *Advance ACS Abstracts,* March 1, 1994.

[1] Abbreviations: GAP, guanosine-5′-triphosphatase activating protein; GDP, guanosine diphosphate; GTP, guanosine triphosphate, GTPase, guanosine-5′-triphosphatase; p21–GTP, 1:1 complex of p21 and GTP; GAP–p21–GTP, 1:1:1 complex of GAP, p21, and GTP; *p21–rap1*, protein product of the Krev-1 gene; p21$^{H\text{-}ras}$, protein product of the Harvey *ras* gene; *rap*1GAP, GAP that naturally activates *p21–rap1*; *ras*GAP, GAP that naturally activates p21$^{H\text{-}ras}$; RMS, root mean square.

0006-2960/94/0433-3237$04.50/0 © 1994 American Chemical Society

basis of X-ray structure analysis of the active site of p21–GTP, that a crystallographic water is activated for head-on nucleophilic attack on the γ phosphate (to form a bipyramidal transition state) by the oxygen of the Gln-61 side chain and the backbone of Thr-35. Additionally, the γ phosphate interacts with the protein through hydrogen bonds to the backbone at Gly-60 and Thr-35 as well as the side chain of Lys-16. On the other hand, Prive et al. (1992), who observe a different space group and packing than Pai et al. (1990), propose a model of the transition state in which both functional groups of the side chain of Gln-61 act to stabilize the transition state involving a hydroxide ion attacking the γ phosphate. The other protein–γ-phosphate interactions are the same as those of Pai et al. (1990). Prive et al. (1992) argue that the activation of water by the side chain of Gln-61 is not reasonable, citing experimental work (Der et al., 1986) that apparently showed that the Q61E mutation, as well as the Q61L mutation, have lowered hydrolysis rates (by 90%) compared to the wild type. Also, they argue that Gln-61 is a poor base and would not be able to "activate" a critically positioned water. A similar conclusion has been reached in the empirical valence bond studies of Langen et al. (1992), in which the theoretically determined activation energy is too high to account for the measured reaction rate constant. Finally, recent work by Chung et al. (1993) using unnatural amino acids engineered at position 61 have shown that some residues with functional groups that would be predicted to be very poor bases still have normal intrinsic hydrolysis rates.

In this paper, we address several issues regarding the involvement of the residue 61 side chain in the intrinsic hydrolysis event. First, we have reexamined experimentally the question of the intrinsic hydrolysis rate of the Q61E mutant. Is the intrinsic hydrolysis rate of Q61E slower than wild type, as found by Der et al. (1986), or is it faster than wild type, as would be expected if the 61 residue is involved in activating the catalytic water molecule? The glutamate side chain is a much stronger base than the glutamine side chain and would therefore be expected to provide an increased activation rate if, in fact, the side chain of residue 61 is acting as a general base. Second, we have performed lengthy molecular dynamics simulations on different p21 proteins (wild type, G12P, G12V, G12R, Q61L, and Q61E) for which experimental studies exist, to investigate the dynamical properties of the residue 61 side chain and whether such studies are in support of the biochemical properties of these proteins.

MATERIALS AND METHODS

Cloning Techniques and Mutagenesis. Restriction endonucleases and T4 DNA ligase were from Boehringer Mannheim, FRG. They were used as described in the laboratory manual of Sambrook et al. (1989). M13 ds DNA containing mutated (Q61E) H-*ras* cDNA was prepared using a clone supplied by C. Der. It was digested with *Pvu*II and *Nco*I and ligated into the corresponding fragment from the expression vector ptac-rasC (John et al., 1988). The sequence of the insert was verified by DNA sequencing using the T7 polymerase kit from Pharmacia. The *Escherichia coli* strain CK600 was used as a host, which is K12 wild-type CK600 containing the plasmid pDMI.1 (Certa et al., 1986) carrying the *lacI*^{q} gene and a kanamycin resistance gene (K). This plasmid is compatible with the expression plasmid.

Protein Purification. Protein purification was performed essentially as described previously (Tucker et al., 1986; John et al., 1988): due to the instability of the p21(Q61E) variant, all buffers contained 10% glycerol, which stabilized the protein from denaturing since it no longer precipitated from solution and did not rapidly lose activity. The final purity of the protein was >95%, as judged from sodium dodecyl sulfate–polyacrylamide gel electrophoresis. It was also possible to stabilize the protein with excess nucleotide. Protein concentrations were determined with the Bradford assay using bovine serum albumin as standard (Bradford, 1976) while [8-^{3}H]GDP binding activity was determined by the filter binding assay (Tucker et al., 1986). Protein was shock-frozen by liquid nitrogen and stored at −70 °C in 64 mM sodium azide and 20% glycerol. The above concentration of the protein immediately after thawing was 190 μM measured by GDP binding.

Nucleotide Dissociation Rates and Relative Affinities for Guanine Nucleotides. The rates of dissociation of [8-^{3}H]-GDP and [^{32}P]GTP from the p21 nucleotide complex were measured with the filter binding assay as described previously (John et al., 1988). Nitrocellulose filters from Schleicher and Schüll (BA 85, pore size = 0.45 μm) were used. The reaction conditions were 1 μM p21(Q61E), 64 mM Tris-HCl, pH 7.6, 1 mM dithiothreitol, and 1 mM sodium azide, reaction volume 1 mL, temperatures 21 and 37 °C. The protein was loaded with the radioactively marked nucleotide in the presence of 1 mM EDTA. The $MgCl_2$ was brought to 10 mM and the reaction was started by adding respectively 1 mM GDP or 1 mM GTP. The decay of the bound radioactivity was followed by a filter binding assay. The kinetics in the absence of $MgCl_2$ were done with a fluorescent analog of GDP, *N*-methylanthraniloyl-GDP (mantGDP). To a preformed complex of either p21(Q61E)·GDP or p21(Q61E)·GTP was added an excess of mantGDP, and the change in the fluorescence signal was recorded. The experiments were performed in a stopped-flow apparatus (High Tech Scientific, Salisbury, U.K.). Excitation of fluorescence of mantGDP was at 366 nm, and detection was through a filter with a cutoff at 445 nm. The relative affinities were measured as the inhibition of the [8-^{3}H]-GDP binding by increasing amounts of the different guanine nucleotides. To 1 μM p21(Q61E) and 10 μM GDP in 60 mM Tris-HCl, pH 7.6, 1 mM EDTA, 1 mM dithiothreitol, and 1 mM sodium azide were added increasing concentrations of GTP or GTPγS. After incubation for 3 h at 0 °C, $MgCl_2$ was added to an end concentration of 10 mM and the filter-bound radioactivity was determined.

GTPase Activity. The intrinsic GTPase activity measurements were not made with the preformed p21–GTP complex as described previously (Reinstein et al., 1991). Due to the high dissociation rates for the guanine nucleotides of p21-(Q61E) it is not possible to measure the hydrolysis of GTP with the filter binding assay. The necessity of always having excess nucleotide in the solution suggests measurement of P_i release. The rates of P_i production were determined in independent experiments with increasing GTP concentrations ranging from 0.02 up to 2 mM. Briefly, this was done by incubating 5 μM p21(Q61E)·GDP in 64 mM Tris-HCl, pH 7.6, 10 mM $MgCl_2$, 1 mM dithiothreitol, 1 mM sodium azide, and 0.5% glycerol at 37 °C in a final volume of 1 mL. Control experiments with wild-type p21 have shown that the addition of up to 10% glycerol does not have any influence on the intrinsic GTPase (data not shown). The reaction was started by the addition of the appropriate amount of GTP. At defined time intervals, 100-μL aliquots were removed and the production of ^{32}P was measured as described (Leupold et al., 1983). For the determinations of the apparent dissociation constants for GTPγS, the production of ^{32}P was monitored at fixed GTP concentrations of 20, 40, and 100 μM. But the GTP hydrolysis was inhibited by increasing concentrations of

Table 1: Summary of Dissociation Rate Constants for Guanine Nucleotides of p21(Q61E)

	21 °C, 1 mM EDTA, 1 μM $MgCl_2$ (min^{-1})	21 °C, 10 mM $MgCl_2$ (min^{-1})	37 °C, 10 mM $MgCl_2$ (min^{-1})
GDP	2.2	0.13	1.0
GTP	24.6	0.24	
GTPγS		0.26	

GTPγS up to 2 mM. GTPase measurements in the presence of GAP were done in the GAP reaction buffer: 20 mM Hepes·NaOH, pH 7.5, 2 mM $MgCl_2$, and 1 mM dithiothreitol with 20 μM p21(Q61E) and 0.5 μM GAP in a final volume of 1 mL at 25 °C. The released P_i was detected as mentioned above. The GAP was prepared as described earlier (Gideon et al., 1992). The experimental data were fitted with the program GraFit, Erithacus Software Limited.

Molecular Dynamics. Essentially the same techniques as were employed by Foley et al. (1992) were used. The molecular modeling program AMBER 3.0a was employed with the modifications outlined in Foley et al. (1992). Additionally, hydrogens were set to mass 1.0 amu and the nonbonded interactions were updated every 10 steps (1 step/fs). Great care was taken to place and equilibrate solvent and counterions and integrations were carried out until the RMS deviation from the starting structure became relatively constant. The starting wild-type coordinates were provided by the 1.35-Å structure of Pai et al. (1990), in which the Gln-61 side chain is oriented away from the γ phosphate region. The Q61E mutant was prepared by direct modification of the Gln61 side chain using the wild-type crystal structure. For all simulations, GTP, rather than analogs, was used in the nucleotide pocket.

RESULTS AND DISCUSSION

Biochemical Properties of p21(Q61E). The p21 mutant (Q61E) was created by site-directed mutagenesis and expressed in *E. coli* using the expression plasmid ptac-ras described earlier. However, the purification of the protein p21(Q61E) was accompanied by a loss of protein due to the decreased stability of this protein. We could stabilize the protein by using glycerol during purification and storage and by keeping protein saturated with guanine nucleotides. The instability is possibly due to the extra negative charge located close to the phosphate residues of GDP/GTP. Altogether there are now three glutamic acids (Glu-61, -62, and -63) near the active site. Hence the biochemical properties of p21(Q61E) are dramatically altered as compared to wild type. The additional carboxylate clearly weakens the binding of the guanine nucleotides. The dissociation rate constants at 21 °C in the presence of Mg^{2+} for GDP and GTP (shown in Table 1) are increased more than 100-fold (7.0×10^{-4} min^{-1} for wild type vs 0.13 min^{-1} for Q61E).

Using different concentrations of GTP we noticed that the GTPase rate increases with increasing GTP concentrations. The high dissociation rate of 1 min^{-1} ($t_{1/2}$ = 42 s, 37 °C, 10 mM Mg^{2+}) for the product GDP suggests the measurement of GTPase activity of this mutant under turnover conditions. Figure 1 shows that the enzymatic reaction of the mutant is only saturated with millimolar concentrations of GTP and gives a K_M of 152 μM and a k_{cat} of 0.57 min^{-1}. Thus, under saturating concentrations the GTPase is approximately 20 times faster than the single-turnover reaction of the wild-type p21 with a rate constant of 0.028 min^{-1} (Krengel et al., 1990). However, the GTPase reaction could not be activated by GAP despite a GAP binding affinity comparable to that of the

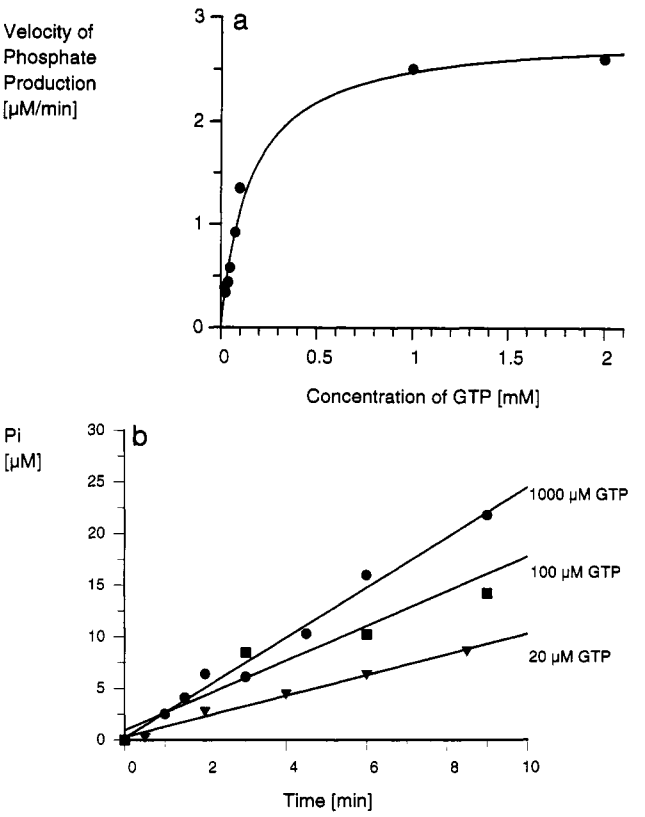

FIGURE 1: GTP hydrolysis by p21 Q61E. Protein (5 μM) (isolated as the GDP complex) was incubated with various concentrations of GTP as indicated and the rates of hydrolysis were measured at 37 °C as described in Materials and Methods. (a) The Plot of the reaction rate vs GTP concentration was fitted to the Michaelis–Menten equation with K_M = 152 μM and k_{cat} = 0.57 min^{-1}. (b) Product vs time plots at various substrate (GTP) concentrations.

Table 2: Comparison of Kinetic and Biological Properties of p21 and Its Mutants

	intrinsic hydrolysis rate constant ($min^{-1} \times 10^{-3}$)	GAP activation	transforming activity
wild type	28.0[a]	+	–
G12P	43[b] (55)[c]	+	–
G12V	2.0[a]	–	+
G12R	1.4[a]	–	+
Q61L	1.3[a]	–	+
Q61E	570.0[d]	–	–

[a] Krengel et al. (1990). [b] Franken et al. (1993). [c] Gibbs et al. (1988). [d] This study.

wild-type protein (Table 2). Even under high concentrations of GAP and p21(Q61E) where the GTPase of the wild type is maximally stimulated (k_{cat} = 20 s^{-1}) there is no effect (data not shown).

The dependence of the GTPase reaction on the GTP concentration up to the millimolar concentration range and the high nucleotide dissociation rates suggest an unusually low affinity for GTP. Reliable affinity constants for guanine nucleotide binding proteins can only be obtained using dissociation and association rate constants (Goody et al., 1991). But for this mutant protein the association rate constant using nucleotide-free p21(Q61E) prepared by the method used from John et al., 1990 could not be determined due to the protein instability in the absence of nucleotide. Therefore, we estimated the affinity by an indirect procedure. The high exchange rates for the nucleotides make it possible to inhibit the GTP hydrolysis of p21(Q61E) by GTPγS in a competitive manner. By increasing concentrations of GTPγS we were able to inhibit the hydrolysis completely (Figure 2a). The

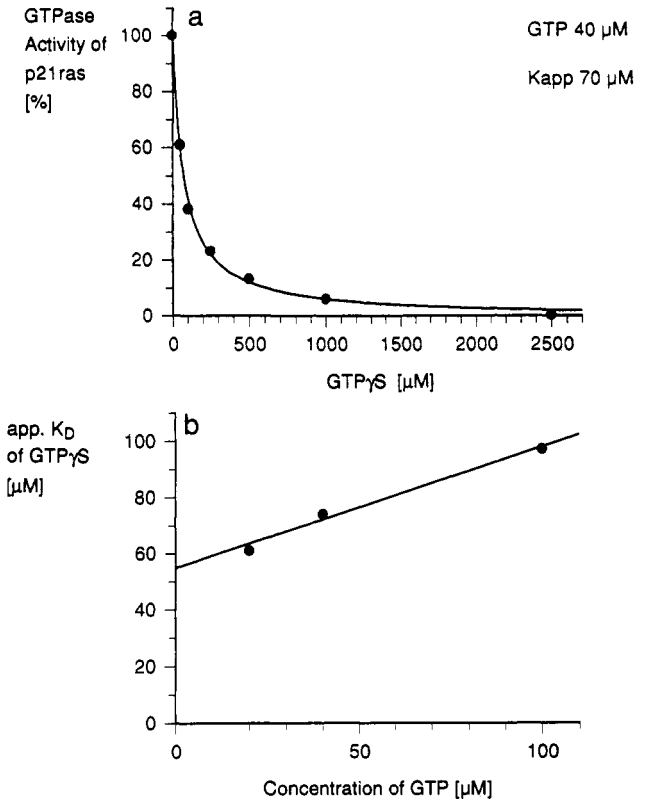

FIGURE 2: (a) Inhibition of the p21 Q61E GTPase reaction by GTPγS. GTPase reaction rates with 5.0 μM protein, a fixed concentration of GTP, and increasing concentrations of GTPγS were measured as described in Materials and Methods. The apparent inhibitor constants were replotted (b) as described in Results to determine the K_d for GTP (115 μM) and GTPγS (52 μM).

apparent inhibition constant obtained is a linear function of the GTP concentration with the intercept giving the dissociation constant of GTPγS and the slope corresponding to the ratio K_D(GTPγS)/K_D(GTP). A replot (Figure 2b) of the data gives a dissociation constant for GTP of 115 μM and for GTPγS of 52 μM. The same relative dissociation constants could be seen by measuring the relative affinities of GTP and GTPγS versus GDP. Here we found a relative affinity of 0.24 for GTP versus GDP and 0.5 for GTPγS versus GDP, indicating that GTP has a 2-fold lowered affinity compared to GTPγS. In summary, the affinity for guanosine triphosphates is indeed very low. Compared with the known binding data of the wild-type p21 *ras* protein (John et al., 1990), the dissociation constant is enlarged by 8 orders of magnitude. Considering that the nucleotide dissociation rates are about 2 orders of magnitude faster than for the wild-type protein, the association of the nucleotide with the mutant protein is consequently influenced drastically.

The fact that the GTPase reaction is not accelerated by GAP suggests that p21(Q61E) could be a transforming protein. Furthermore, *ras* proteins that exhibit high guanine nucleotide dissociation rates are transforming. For this mutant, however, it is possible that the lifetime (estimated $t_{1/2} \approx 26$ s) of the active GTP complex is too short to transmit a growth promoting signal. The kinetic data, high GTP dissociation rate, high GTP hydrolysis, and 4 times lower affinity for GTP than for GDP suggest a protein which is not transforming or only very weakly transforming. We tested the activity of the mutant in PC12 cells, which provides an indication of its biological activity in other cell systems such as transformation of fibroblasts. We could not detect a biological activity with this assay which is significantly greater than the one produced by the wild-type protein. A weakly transforming activity, however, has been found by transfection of the mutant cDNA into rat fibroblasts (C. Der, unpublished observation). It is not known how this protein interacts with a guanine nucleotide exchange factor and whether the exchange factor can activate this mutant. The instability of the protein *in vivo* may also be a contributing factor.

General Features of the Wild-Type and Q61E Simulation Structures. Molecular dynamics provides a methodology for studying the dynamic behavior of macromolecular systems in atomic detail. The procedure outlined in the Material and Methods section and in Foley et al. (1992) was used to examine the dynamic behavior of the wild-type and Q61E proteins using the X-ray crystal structure to define the starting positions. In both cases the side chain of residue 61 is initially directed away from the γ phosphate.

The simulations were carried out until the RMS deviation from the starting structure became essentially constant. The average RMS deviation (over all backbone atoms) for the simulation of the wild type was approximately 1.6 Å for the 130–150-ps average structure and 1.9 Å for the 230–250-ps average structure of the Q61E simulation. The Q61E simulation was carried out twice as long (400 ps) as the wild type (200 ps) simulation to ensure equilibration. Protein–nucleotide contacts are given in Table 3. The γ-phosphate group in the simulation structures retains its H-bonds with the backbone NHs of Thr-35 and Gly-60. Likewise, the side-chain hydrogen bonds of Lys-16 with both the γ- and β-phosphate groups which are seen in the crystallographic structure are also present in the simulation structures. The immediate environment around the Mg^{2+} ion does not change in either simulation; the side chains of Thr-35 and Ser-17, oxygens from the γ- and β-phosphate groups, and two water molecules remain fixed to the Mg^{2+}. If the average simulation backbone structures are compared (minus the regions of expected change: 1–10, 61–68, and 157–166) to the crystallographic structure using the RMS deviation of the α-carbons, it is clear that there is substantial motion in the region of the termini and residues 61–68, with the latter region giving an average difference of 2.62 Å for the wild type and 1.99 Å for the Q61E simulation. On the other hand, the same comparison gives several regions of low change relative to the crystal structure: for residues 11–23 (an average of 0.534 Å for the wild type and 0.714 Å for Q61E) and for residues 111–120 (an average of 0.794 Å for the wild type and 0.497 Å for the Q61E simulation). These two regions are intimately involved in securing the GTP in place.

A comparison of the secondary structures (helix and beta sheets) as determined by the Kabsch and Sander algorithm (1983) is given in Table 4. There is considerable similarity in the assignment of secondary structure, particularly in regions 16–24, 127–137, 142–163 (all helixes), and 77–85 (β sheet); the assignment is identical for all three structures in these regions. On the other hand, the N-terminal β sheet and the antiparallel β sheet (~38–57) for Q61E show some change compared to the crystal structure. The latter observation is consistent with an NMR study of the wild-type protein (Yamasaki et al., 1989). Likewise, the first several residues of the helix immediately after the hyperflexible loop (residues 61–65) show variation for the Q61E simulation. In summary, over 90% of the residues of the X-ray crystal structure that are assigned to a secondary structure retain that assignment in the wild-type and Q61E simulations.

Mechanism of Hydrolysis. As outlined in the introduction, a key question centers on the intrinsic hydrolysis rate of the Q61E mutant protein. Der et al. (1986), have reported that the rate for this mutant is decreased significantly relative to

Table 3: Significant Protein–GTP Contacts[a]

interactions	X-ray[b]	wild type (130–150 av)	Q61E simulation (230–250 av)
Mg^{2+}	γ- and β-phosphate, 2 waters, T35, S17	γ- and β-phosphate, 2 waters, T35, S17	γ- and β-phosphate, 2 waters, T35, S17
γ-phosphate	Mg^{2+}, G13, K16, T35, G60	Mg^{2+}, [G13], K16, [T35], G60	Mg^{2+}, K16, T35, G60
β-phosphate	Mg^{2+}, G13, G15, K16, S17	Mg^{2+}, G13, [V14], G15, K16, S17	Mg^{2+}, G13, [V14], G15, K16, S17
α-phosphate	A18	[G15], A18	[G15], [S17], A18
ribose	V29, D30, [K117]	[K117]	D30
guanine	N116, D119, A146	N116, D119, [S145], A146, K147	N116, D119, [S145], A146, K147

[a] The criterion for a hydrogen-bonded contact is O,N–N,O < 3.5 Å and [O,N]–H < 2.4 Å. Contacts shown in brackets indicate a near contact, usually the longer criterion met but not the shorter. Ionic contact criterion: <2.5 Å. The water molecules bound to the Mg ion are identical to those of the crystallographic structure. [b] Pai et al. (1990).

Table 4: Secondary Structure Using the Kabsch–Sander (1983) Algorithm[a]

Seq. No.	1 2 3 4 5 6 7 8 9 0 1 2 3 4 5 6 7 8 9 0 1 2 3 4 5 6 7 8 9 0 1 2 3 4 5 6 7 8 9 0 1 2 3 4 5 6 7 8 9 0 --50
X-ray	E E E E E E E E T T H H H H H H H H H E E E E E E E E E E E E E
Wild Type	E E E E E E T T H H H H H H H H H T E E E E E E E E E E T T E E
Q61E	E E E E E T T H H H H H H H H H T E E E E E E E T T E E

	1 2 3 4 5 6 7 8 9 0 1 2 3 4 5 6 7 8 9 0 1 2 3 4 5 6 7 8 9 0 1 2 3 4 5 6 7 8 9 0 1 2 3 4 5 6 7 8 9 0 --100
X-ray	E E E E E E E E T T H H H H H H H E E E E E E E E T T H H H H T T H H H H H H H H
Wild Type	E E E E E E E E H H H H H H H E E E E E E E E T T H H H H H H H H H H H H H H H H
Q61E	E E E E E E E H H H H H H H H H E E E E E E E E T T H H H H T T H H H H H H H H

	1 2 3 4 5 6 7 8 9 0 1 2 3 4 5 6 7 8 9 0 1 2 3 4 5 6 7 8 9 0 1 2 3 4 5 6 7 8 9 0 1 2 3 4 5 6 7 8 9 0 --150
X-ray	H H H T T E E E E E E T T H H H H H H H H H H T E E E T T T T
Wild Type	H H H H E E E E E E T T H H H H H H H H H H T E E E T T T T
Q61E	H H H H E E E E E E T T H H H H H H H H H H T E E E T T T T

	1 2 3 4 5 6 7 8 9 0 1 2 3 4 5 6 --166
X-ray	T H H H H H H H H H H H H H T
Wild Type	H H H H H H H H H H H H H H
Q61E	H H H H H H H H H H H H H T

[a] E = β sheet, H = helix, T = hydrogen-bonded turn. Wild type = 130–150 ps average; Q61E = 230–250 ps average.

the wild type. However, the side chain of glutamate would normally be a considered a stronger base than that of glutamine. Consequently, we have further investigated the kinetic properties of the Q61E mutant. We find that the intrinsic hydrolysis rate of Q61E is actually elevated relative to that of the wild type. The reason for the discrepancy between the Der et al. (1986) result and ours is that substrate concentrations greater than those used in the Der et al. study (1986) are required to effect a measurable hydrolysis rate. Also, we have found that since the protein is unstable, special precautions have to be provided during purification and storage.

A second key question relates to the dynamical properties of the side chains of residue 61 in the wild-type and mutant proteins. If the functional groups of these side chains sample the space around the nucleophilic water (WAT-175) for a significant amount of time, this would lend support to the idea that the side chain of residue 61 is involved in the mechanism. The geometry of the active site according to the crystallographic coordinates (Pai et al., 1990) is shown in Figure 3a. It also shows a crystallographic water molecule in a position suitable for nucleophilic attack (3.7 Å from the γ-phosphate phosphorus) which interacts strongly with the backbone oxygen of Thr-35 but is distant from the side chain O_ϵ of Gln-61. This water molecule remains in this position for essentially the entire time course of the simulation for wild type and Q61E. Figure 3b shows the geometry of the active site at 66 ps in the simulation. The side chain of Gln-61 has moved from its crystal structure position to a position that has a hydrogen-bonding interaction with the well-positioned water molecule. The distances of the water molecule from the γ-phosphorus and from the Q61-O_ϵ atom are shown as a function of simulation time in Figure 4a. The interaction of the Q61 side chain with the nucleophilic water strengthens early in the simulation with substantial oscillation in the latter half. The water molecule retains its interaction with Thr-35. The NH_2 group of the side chain of Gln-61 is occasionally stabilized by an interaction with the side chain of Glu-63 (Figure 4b). Thus, in our hands, the Q61 side chain appears to have considerable positional flexibility and has a certain probability of being near the nucleophilic water. These results are consistent with an intrinsic hydrolysis mechanism for which the side chain of residue 61 is involved.

We draw essentially the same conclusions from the Q61E simulation. Figure 3c shows a snapshot of the active-site geometry after 198 ps of simulation. As observed in the wild-type simulation, a water is well-positioned for attack on the γ phosphate; this water is hydrogen-bonded to the backbone oxygen of Thr-35 and to the side chain O_ϵ of Glu-61. Figure 4b examines the dynamics of the water interaction with the γ-P and the side chain of Glu-61. Clearly the water remains near the γ-P for the entire 400 ps. The Glu-61 side chain, which is initially oriented away from the nucleophilic water, moves into hydrogen-bonding position with the water very early in the simulation and then shows an oscillatory interaction for the remainder of the simulation. The interaction is stable for approximately 70% of the simulation. An interaction seen in the wild-type simulation between the side chains of residues 61 and 63 is not likely here due to charge repulsion.

Figure 4c shows that the Thr-35 backbone O interaction with the critical water is also mostly stable for the length of the wild-type simulation. Figure 4d shows that the behavior of this interaction for the Q61E mutation is similar to the wild type. Thus, a water molecule is essentially locked in position

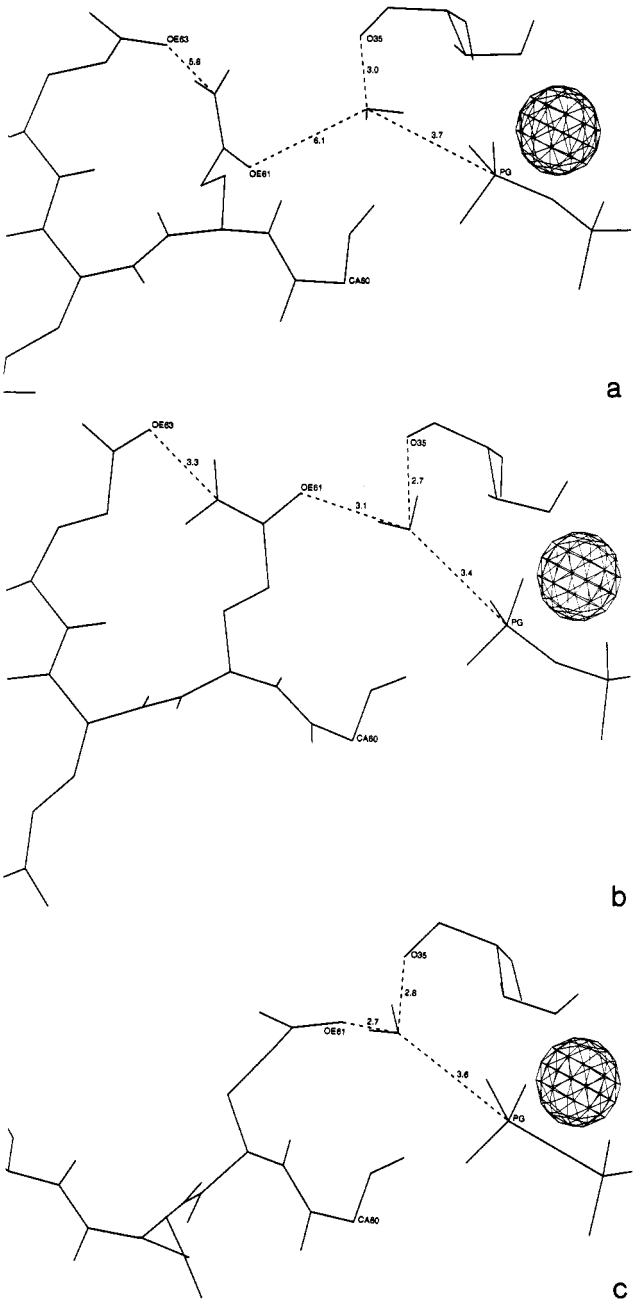

FIGURE 3: Active-site region for the hydrolysis of GTP by p21. (a) X-ray crystal structure of p21; (b) the 66-ps configuration of the wild-type simulation; (c) the 198-ps configuration of the Q61E simulation.

by its hydrogen-bonding interactions with the γ-phosphate, the backbone oxygen of T35, and the side chain of E61 (carboxylate oxygen), and this water is potentially a candidate to perform the in-line hydrolysis as it is polarized by its interactions.

We have also carried out long simulations on the other mutants of $p21^{H\text{-}ras}$. A control simulation, G12P, was performed since this mutation shows kinetic properties very similar to the wild type. The crystallographic coordinates of Franken et al. (1993) were used. We find that the Gln-61 side-chain O_ϵ and the O_γ of Thr-35 are able to assume, at certain times, the complex involving the γ-phosphate, a water molecule, the backbone of T35, and the O_ϵ of the side chain of Q61. For the G12V mutant, made by modeling in the added Val-12 side chain before beginning the simulation, we find that although a water molecule can adjust into the γ-phosphate region, the side chain of Q61 is unable to interact with the water in the manner that we have seen for the wild-type and Q61E simulations. Also, the hydrogen bond of the water molecule with the backbone of T35 is considerably weakened so that eventually this water molecule leaves the active site (~110 ps). Figure 5 shows the active-site region for the G12V mutant protein after 105 ps. A simulation of G12R, which utilized the Krengel et al. (1990) crystallographic structure for starting coordinates, showed that the tight salt bridge between the side chain of the Arg-12 group and the γ-phosphate persisted throughout the simulation and thus partially blocked the hydrolysis. Finally, a simulation performed on the highly transforming Q61L mutation, using the crystallographic coordinates (Pai et al., 1990), was carried out. Other than the backbone oxygen of T35, the water molecule nearest the γ-phosphate has no activating contacts throughout the simulation. Thus, the simulations on these other mutations are encouraging. The only simulation that gives a transient structure similar to those of the wild type and Q61E is the G12P simulation, and this mutation is the one whose intrinsic hydrolysis rate is most similar to the wild type and the Q61E mutant.

That Gln-61 is indeed involved in the hydrolysis is supported by other lines of investigation. The *p21–rap1* proteins have greater than 50% sequence identity (Polakis & McCormick, 1992) to $p21^{H\text{-}ras}$ and are essentially identical in the region involved in GTP binding. *P21-rap1* has a Thr at position 61 and, although the protein is sensitive to its own GAP (*rap*1GAP), which greatly increases the hydrolysis rate, it is insensitive to *ras*GAP. Frech et al. (1990a) made the mutation T61Q in *p21–rap1* and consequently showed that this mutation increases its intrinsic hydrolysis rate and renders it insensitive to *ras*GAP. Previously, Maruta et al. (1991) had shown that the rapGAP stimulation of Rap1p21 was unaffected by the T61Q substitution. Thus, the side chain of Q61 may interact directly with one or more groups on *ras*-GAP. In the active conformation proposed by Pai et al. (1990), the O_ϵ and NH_2 groups of the Q61 side chain are both at the surface of the protein.

The *rap*2 protein also with a threonine at position 61 has a low GTPase activity as well (Lerosey et al., 1991). Furthermore, the substitution of the homologues Gln by Leu in the *ral*A protein lead to a 2-fold decrease in the GTPase activity (Frech et al., 1990b) and cannot be activated by the *ral*GAP (Emkey et al., 1991). Although this substitution has only a weak effect for the *ral* protein, the activation by GAP is greatly impaired as it is found for the *ras* proteins.

We have shown here that Q61E may adopt an orientation of its side chain which is close to the nucleophilic water molecule. Since the carboxylate side chain of glutamic acid has a much higher pK_a than the carboxamide side chain of glutamine, it should be much more able to act as a general base in the possible activation of the nucleophile. The fact that the intrinsic hydrolysis rate of p21(Q61E) is 20 times higher than that of wild-type p21 lends qualitative, if not quantitative, support for a role for Glu-61 in the hydrolysis mechanisms of GTP.

The fact that the intrinsic GTPase activity is not accelerated by GAP need not be in contradiction to this since GAP may either recognize the glutamine 61 residue itself or the proper orientation of the various side chains of loop L4 amino acids, which are certainly perturbed by the presence of the acidic side chain, as can be seen from the drastically different biochemical properties of this mutant (Table 2). Thus the juxtaposition of Gln-61 and Glu-63 for which we see evidence in the dynamics simulations for the wild type may be important in the mechanism of either the intrinsic and/or the GAP-

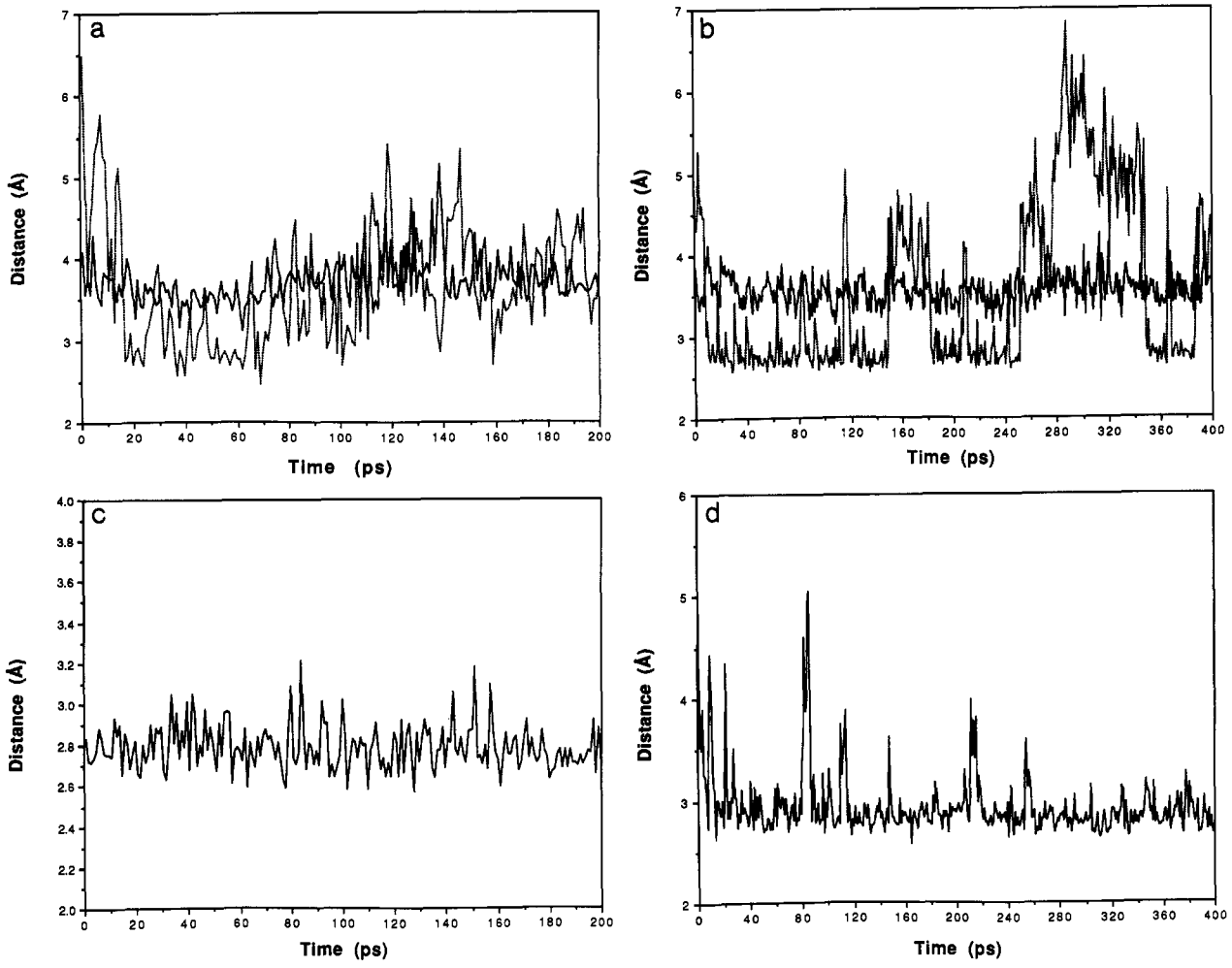

FIGURE 4: Time profiles of key distances in the activated water complex. (a) Wild-type simulation. Water–γ P distance (solid line); water–O_ϵ(Q61) distance (dotted line). (b) Q61E simulation. Water–γ P distance (solid line); water–O_ϵ(E61) distance (dotted line). (c) Wild-type simulation. Water–O(T35) distance. (d) Q61E simulation. Water–O(T35) distance.

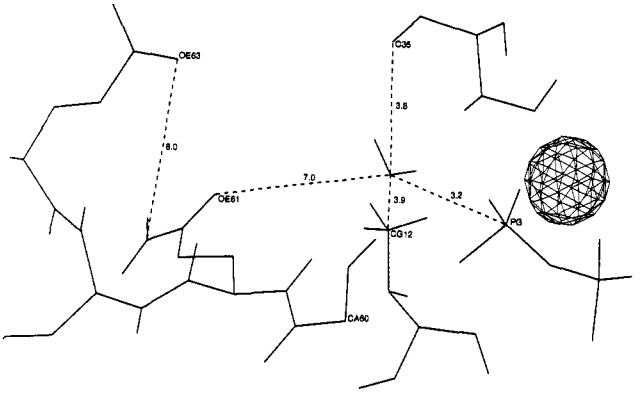

FIGURE 5: Active-site region for the G12V simulation at 105 ps.

mediated hydrolysis mechanism. The inability of GAP to stimulate GTP hydrolysis by p21(Q61E) may also be an argument for the hypothesis that the chemical and/or kinetic mechanism for the GAP-mediated reaction may in fact be different. In the mechanism proposed by Prive et al. (1992), the glutamine does not act as a general base but rather is involved in the stabilization of the transition state involving the pentacoordinate phosphorus via both the carbonyl and the amido part of the glutamine side chain. The experiments described above as well as those of Chung et al. (1993) make such a role for residue 61 implausible since the carboxylate side chain of Glu-61 could not adopt the conformation proposed by Prive et al. (1992), at least for the intrinsic reaction. It is still possible however, that the GAP-catalyzed reaction, which is 10^5 times faster than the intrinsic reaction rate (Gideon et al., 1992), may operate by such a mechanism.

It has been shown by Chung et al. (1993) that the replacement of Gln-61 by an unnatural nitro analog NGln, which is isoelectronic and isosteric with glutamine, or by HGln, an amino acid similar to Gln but with an additional CH_2 in the side chain, does not impair the intrinsic GTPase reaction. The authors have also shown that both the NGln-61 p21^{ras} complex and the HGln-61 p21^{ras} complex are apparently stimulated by GAP, although the exact stimulation of the intrinsic GTPase activity has not been evaluated quantitatively. Since the nitro group has a pK_a value which is 10 log units lower than that of the carboxamide group of Gln-61, it has been interpreted to indicate that Gln-61 is not acting as a general base to active water. The ability to polarize water is very low for either the carboxamide (of Gln-61 or HGln-61) or the nitro side chain of the respective proteins, pointing to the fact that p21-*ras* has a very low GTPase activity in the absence of GAP. Even though not much is known on the dependence of the reaction rate on the pK_a of the base in a general-base-catalyzed enzymatic reaction involving phosphoryl transfer (the Bronsted β value), one would expect that lowering the pK_a of the base by 10 log units should decrease the reaction rate drastically. On the other hand, the data presented hear clearly show that by mutating Gln61 to Glu and thereby increasing the pK_a of the side chain by about 5 orders of magnitude the rate of the reaction is indeed accelerated. The Bronsted value for the expected proton transfer would, however, be so extremely low and would

indicate such a low degree of charge development in the transition state that other explanations than the change in pK_a for the rate increase should not be dismissed.

Thus there is some evidence that suggests a base mechanism (the fact that the Glu-61 mutant intrinsic rate is significantly greater than for the Gln-61 mutant) and some evidence pointing toward a more structural role rather than chemical role for residue 61 (the fact that the NGln-61 mutant intrinsic rate is essentially the same as the wild type). The dynamics calculations suggest that the side chains of both Gln-61 and Glu-61 interact with the key water molecule and that the Glu-61 system has the stronger interaction. This finding could be consistent with either a base or structural role. That the Gln-61, NGln-61, and HGln-61 proteins all have about the same GAP activity, whereas the Glu-61 protein has no discernible GAP activity, may be due to the fact that the former three residues are uncharged (and all have isoelectronic end groups), whereas the latter residue is formally charged. A reasonable mechanism for the intrinsic hydrolysis might be that the key water does in fact transfer a proton but that the transfer is instead to the highly negatively charged phosphate group. Such a reduction of charge would reduce the repulsion between the attacking hydroxide and the γ-phosphate. This proton transfer could be viewed as a low-probability quantum mechanical tunneling event such as has been seen in other enzymatic systems (Cha et al., 1989; Bahnson et al., 1993). The role of the residue 61 side chains in this case would be to temporally and spatially contain the water near the phosphate. In the case of Glu-61, the greater intrinsic rate observed could be due to the more secure containment of the water molecule as seen in the molecular dynamics simulations.

Taken together, the accumulated experimental and theoretical evidence point to a possible role for the side chain of Q61 in the hydrolysis of GTP by $p21^{ras}$. A molecular mechanism that is consistent with the crystallographic data, with the mutational analysis of Der et al. (1986), with the results presented here, with the data of Chung et al. (1992), and with the theoretical studies such as those reported by Langen et al. (1992) has yet to be found.

ACKNOWLEDGMENT

We wish to acknowledge Howard Smith for very able technical assistance, Thomas Schweins for helpful suggestions and control experiments, and K. C. Holmes for continuous support of the p21 project. We wish to thank the Frederick Cancer Center (NCI) for access to their Cray Y-MP, the North Carolina Supercomputing Center for use of their Cray Y-MP during its early testing phase, and Cray Research, Inc. for a generous grant of computer time. L.G.P. wishes to acknowledge NIEHS for making its facilities available through a visiting scientist appointment.

REFERENCES

Bahnson, B. J., Park, D.-H., Kim, K., Plapp, B. V., & Klinman, J. P. (1993) *Biochemistry 32*, 5503–5507.

Barbacid, M. (1987) *Annu. Rev. Biochem. 56*, 779–827.

Bar-Sagi, D., & Feramisco, J. R. (1985) *Cell 42*, 841–848.

Borasio, G. D., John J., Wittinghofer, A., Barde, Y.-A., Sendtner, M., & Heumann, R. (1989) *Neuron 2*, 1087–1096.

Bos, J. L. (1989) *Cancer Res. 49*, 4682–4698.

Bourne, H. R., Sanders, D. A., & McCormick, F. (1990) *Nature 348*, 125–132.

Bourne, H. R., Sanders, D. A., & McCormick, F. (1991) *Nature 349*, 117–127.

Bradford, M. M. (1976) *Anal. Biochem. 72*, 248–254.

Certa, U., Bannwarth, W., Stüber, D., Gentz, R., Lanzer, M., LeGrice, S., Guillot, F., Wendler, I., Hunsmann, G., Bujard, H., & Mous, J. (1986) *EMBO J. 5*, 3051–3956.

Cha, Y., Murray, C., & Klinman, J. P. (1989) *Science 243*, 1325–1330.

Chung, H.-H., Benson, D. R., & Schultz, P. G. (1993) *Science 259*, 806–809.

Der, C. J., Finkel, T., & Cooper, G. M. (1986) *Cell 44*, 167–176.

Downward, J., Riehl, R., Wu, L., & Weinberg, R. A. (1990) *Proc. Natl. Acad. Sci. U.S.A. 87*, 5998–6002.

Emkey, R., Freedman, S., & Feig, L. A. (1991) *J. Biol. Chem. 266*, 9703–9706.

Foley, C. K., Pedersen, L. G., Charifson, P. S., Darden, T. A., Wittinghofer, A., Pai, E. F., & Anderson, M. W. (1992) *Biochemistry 31*, 4951–4959.

Franken, S. H., Scheidig, A. J., Krengel, U., Rennsland, H., Lautwein, A., Geyer, M., Scheffzek, K., Goody, R. S., Kalbitzer, H. R., Pai, E. F., & Wittinghofer, A. (1993) *Biochemistry* (in press).

Frech, M., Jacob, J., Pizon, V., Chardin, P., Tavitian, A., Clark, R., McCormick, F., & Wittinghofer, A. (1990a) *Science 249*, 169–171.

Frech, M., Schlichting, I., Wittinghofer, A., & Chardin, P. (1990b) *J. Biol. Chem. 265*, 6353–6359.

Gibbs, J. B., Schaber, M. D., Allard, W. J., Sigal, I. S., & Scolnick, E. M. (1988) *Proc. Natl. Acad. Sci. U.S.A. 85*, 5026–5030.

Gideon, P., John, J., Frech, M., Lautwein, A., Clark, R., Scheffler, J. E., & Wittinghofer, A. (1992) *Mol. Cell. Biol. 12*, 2050–2056.

Greene, L. A., & Tischler, A. T. (1982) *Adv. Cell Neurobiol. 3*, 373–414.

John, J., Frech, M., & Wittinghofer, A. (1988) *J. Biol. Chem. 263*, 11792–11799.

John, J., Sohmen, R., Fuerstein, J., Linke, R., Wittinghofer, A., & Goody, R. S. (1990) *Biochemistry 29*, 6058–6065.

Kabsch, W., & Sander, C. (1983) *Biopolymers 22*, 2577–2637.

Krengel, U., Schlichting, I., Scherer, A., Schumann, R., Frech, M., John, J., Kabsch, W., Pai, E. F., & Wittinghofer, A. (1990) *Cell 62*, 539–548.

Langen, R., Schweins, T., & Warshel, A. (1992) *Biochemistry 31*, 8691–8696.

Lerosey, I., Chardin, P., de Gunzburg, J., & Tavitian, A. (1991) *J. Biol. Chem. 266*, 4315–4321.

Leupold, C., Goody, R. S., & Wittinghofer, A. (1983) *Eur. J. Biochem. 124*, 237–241.

Maruta, H., Holden, J., Sizeland, A., & D'Abaco, G. (1991) *J. Biol. Chem. 266*, 11661–11668.

Pai, E. F., Krengel, U., Petsko, G. A., Goody, R. S., Kabsch, W., & Wittinghofer, A. (1990) *EMBO J. 9*, 2351–2359.

Polakis P., & McCormick, F. (1992) *Cancer Surveys 12*, 25–42.

Prive, G. G., Milburn, M. V., Tong, L., DeVos, A. M., Yamaizumi, Z., Nishimura, S., & Kim, S.-H. (1992) *Proc. Natl. Acad. Sci. U.S.A. 89*, 3649–3653.

Reinstein, J., Schlichting, I., Frech, M., Goody, R. S., & Wittinghofer, A. (1991) *J. Biol. Chem. 266*, 17700–17706.

Sambrook, J., Firtsch, E. F. & Maniatis, T. (1989) *Molecular Cloning*, 2nd ed., Cold Spring Harbor Laboratory Press, Cold Spring Harbor, NY.

Schlichting, I., Rapp, G., John, J., Wittinghofer, A., Pai, E. F., & Goody, R. S. (1989) *Proc. Natl. Acad. Sci. U.S.A. 86*, 7687–7690.

Spandidos, D. (1989) *Ras Oncogenes*, Plenum Press, New York.

Tucker, J., Sczakiel, G., Feuerstein, J., John, J., Goody, R. S., & Wittinghofer, A. (1986) *EMBO J. 5*, 1351–1358.

West, M., Kung, H., & Kamata, T. (1990) *FEBS Lett. 259*, 245–248.

Wolfman, A., & Macara, I. (1990) *Science 248*, 67–69.

Yamasaki, K., Kawai, G., Ito, Y., Muto, Y., Fujita, J., Miyazawa, T., Nishimura, S., & Yokoyama, S. (1989) *Biochem. Biophys. Res. Commun. 162*, 1054–1062.